A novel thin-layer photoelectrocatalytic (PEC) reactor with double-faced titania nanotube arrays electrode for effective degradation of tetracycline

Jing Bai, Yanbiao Liu, Jinhua Li, Baoxue Zhou*, Qing Zheng, Weimin Cai

School of Environmental Science and Engineering, Shanghai Jiao Tong University, No. 800 Dongchuan Rd, Shanghai 200240, China

ARTICLE INFO

ABSTRACT

A novel thin-layer photoelectrocatalytic (PEC) reactor has been developed and successfully applied to the degradation of tetracycline, a typical pharmaceutical and personal care products (PPCPs), in bulk wastewater treatment. The reactor is designed with double thin-layer in order to increase the A/V ratio (ratio of electrode area and solution volume) and improve the mass transfer as well as the photonic efficiency of the system. The efficiency of organic degradation by the new reactor is much higher in comparison with conventional PEC process under similar treatment conditions. Using $20–120 \, mg \, L^{-1}$ model tetracycline wastewater as the target organics, the PEC removal rate of tetracycline in the reactor reached 96.4–54.8% with a single-side illumination, much higher than that of conventional PEC reactor (about 80.4–14.6%) within 1 h. When the reactor was illuminated from double sides, the treatment efficiency of thin-layer reactor was doubled without increasing new electrodes. This novel reactor always keeps high quantum efficiency regardless of the different concentration levels of the organic compounds, especially superior for the treatment of high concentration solutions. Repeated experiments in the treatment of $400 \, mg \, L^{-1}$ tetracycline solution demonstrated excellent stability and reliability of the TNAs electrode.

1. Introduction

Photocatalytic (PC) and photoelectrocatalytic (PEC) oxidation by titanium dioxide (TiO_2) has been demonstrated to be an inexpensive and a promising alternative technology for the treatment of wastewater with refractory and toxic organic pollutants [1–3]. In practice, there are two key factors affecting the overall treatment efficiency of a typical TiO_2-based PEC process: (a) the TiO_2 photocatalyst and (b) the configuration of reactor. In the study of TiO_2 catalysts, many efforts have been made to improve the photocatalytic capability of TiO_2 including synthesizing new TiO_2 structures [4–6] or modifying TiO_2 with other elements or compound [7–9]. Recently, the new kind of Ti-foil-based TiO_2 nanotube arrays (TNAs) [10–16] electrodes have attracted considerable attention owing to its unique microstructures. In the TNAs, the well-aligned nanotubes are perpendicular to the electrically conductive Ti substrate, forming a Schottky-type contact naturally and providing a unidirectional electric channel for the transport of photogenerated electrons. When a positive bias is applied across the TiO_2 photoanode, excellent properties of separation of photogenerated electron-hole pairs offer it superior photochemical reactivity over TiO_2 nanoparticulate electrode in the photoelectrocatalysis (PEC)

[17–22]. In our previous work, we have reported the preparation of highly ordered TiO_2 nanotube arrays or nanopore arrays with different morphological characteristics, and applied them as photoanodes in photoelectrochemical applications such as water splitting, organic pollutant degradation and COD determination, etc. [23–30].

On the other hand, the treatment efficiency is also affected by the configuration of reactor; however, the relevant studies are pretty less in comparison to those on the TiO_2 photocatalyst. The reactors were mostly designed to two types, including slurry reactors and immobilized reactors [31–37]. As one of typical immobilized PEC reactor, rotating disc reactor/drum reactor is of certain interest, in which a thin water film between the light source and photocatalyst is formed. Recently, Xu et al. [38] developed a rotating disc reactor for dye wastewater treatment, which was reported to possess enhanced mass transfer properties and treatment efficiency. In that work, TiO_2 nanoparticulate/Ti electrode was used as round disk photoanode, and the upper half of the round disk photoanode was coated with a thin layer of wastewater and exposed to UV radiation in air, meanwhile, the other half of the disk electrode was immersed in bulk wastewater to perform conventional treatment. The reaction was carried out in an open system, the high PEC efficiency was achieved by only half area of the electrode. This kind of reactor was further developed to a Cu–TiO_2/Ti dual electrode oxidation process in their latest report [39].

* Corresponding author. Tel.: +86 021 54747351; fax: +86 021 54747351.
E-mail address: zhoubaoxue@sjtu.edu.cn (B. Zhou).

Thin layer cell technology can greatly reduce the loss of irradiation intensity and facilitate the rapid mass diffusion by offering a thin water film. The application of such technology into reactors enlarges the ratio of TiO$_2$ electrode area and organic solution volume so that organic mass can be degraded rapidly. Zhao et al. [40,41] have applied the thin layer cell technology and TiO$_2$ nanoparticulate electrode into chemical oxygen demand (COD) determination and kinetics study of PEC process. During these processes, the exhaustive redox reaction can be completed in very short time. In our recent work [24,25], we also reported that the TNAs-based COD sensor for rapid and accurate COD determination of wastewater. However, it is evident that this technology cannot be applied into bulk wastewater treatment because of its small cell volume (only 0.785 μL).

A powerful and energy efficient PEC reactor for wastewater treatment should ideally possess: (1) a large catalyst surface area per unit reactor volume, (2) sufficient mass transfer capacity between the liquid bulk and the reaction sites, (3) effectively making use of photons, (4) excellent photoanode for fast electron transfer. In the present work, we combined these advantages to develop a novel thin-layer PEC reactor with double-faced titania nanotube arrays electrode for the highly effective degradation of organic compounds. The reactor was designed with double thin-layer configuration in order to increase the A/V ratio (ratio of electrode area and solution volume) and improve the mass transfer as well as the photonic efficiency of the system. Furthermore, a relatively closed design in the reactor can prevent organic pollutant from evaporation into air during the operation. The feasibility of the reactor was demonstrated by the treatment of model tetracycline wastewater. Then the reaction kinetics was analyzed experimentally and mathematically. Important factors were also discussed. Fig. 1 presents the UV–visible spectra and molecular structure of tetracycline (TC), which is a typical pharmaceutical and personal care products (PPCPs) [42,43].

2. Experimental

2.1. Materials

Pieces of titanium (Ti) sheets (purity > 99.99%) were purchased from Kurumi works, Japan. Tetracycline hydrochloride (C$_{22}$H$_{24}$N$_2$O$_8$·HCl, see Fig. 1a), hydrofluoric acid, sodium sulfate, sodium hydroxide, and acetone were obtained from Shanghai Chemical Reagent Company (China) without further purification. All solutions were prepared with doubly distilled deionized water.

2.2. Preparation of double-faced TNAs electrode

The doubled-faced TNAs electrodes was prepared by using a modified route of electrochemical anodization reported by Gong [10] and our previous work [23]. In a typical fabrication process, the titanium sheets were cleaned with acetone in an ultrasonic bath, followed by rinsing in deionized water and finally drying in air. The doubled-faced TNAs electrodes (40 mm × 50 mm × 0.1 mm or 80 mm × 50 mm × 0.1 mm in dimension) were grown by potentiostatic anodization at 20 V using a platinum cathode (area: 40 mm × 40 mm) in 0.5 wt% HF solution for 1 h. During the fabrication, the front side of the electrode is facing the platinum cathode, and the other surface is the back side. Then the resulting double-faced TNAs electrode were annealed in the air ambience at 500 °C for 3 h; heating and cooling rates were kept at 1 °C min^{-1}.
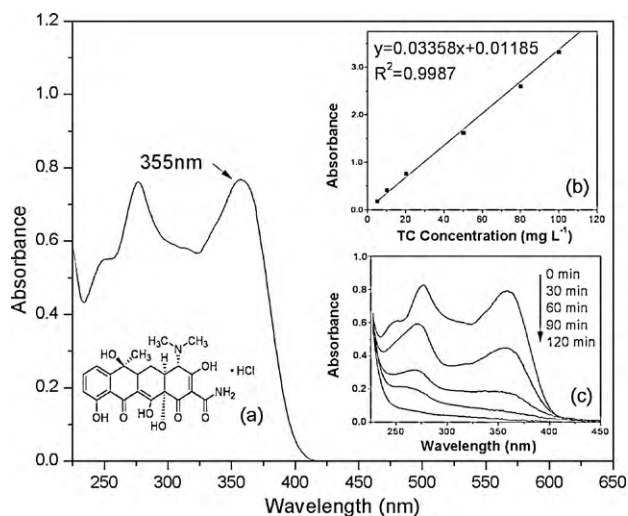
2.3. Characterization of TNAs electrode

The surface morphology of TNAs was investigated by field emission scanning electron microscopy (FE-SEM FEI-Sirion200) under voltage of 5 kV, and the crystal patterns of TNAs were characterized by X-ray diffractometer (XRD, Bruker D8) using a Cu target at the scan rate of 4 deg min^{-1}.

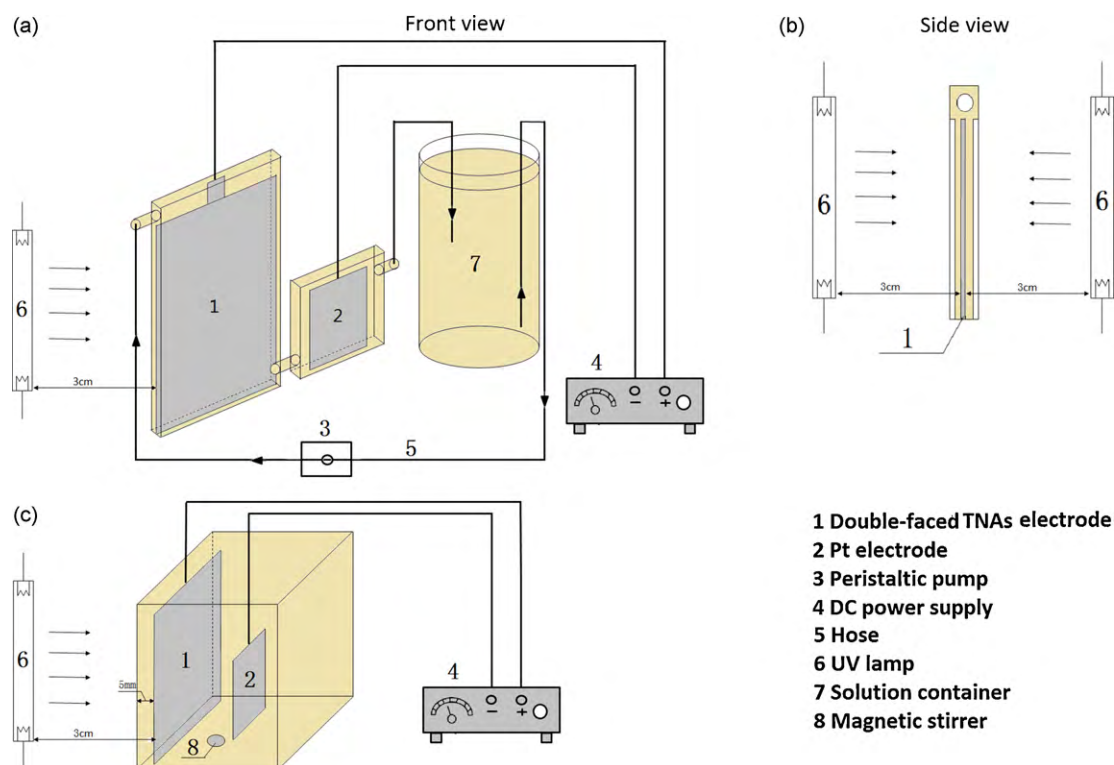### 2.4. The double-faced TNAs electrode based thin-layer PEC reactor

The double-faced TNAs electrode based separate type thin-layer PEC reactor consists of two interconnected quartz cells: one cell was 40 mm × 50 mm × 0.5 mm in net dimension with a 40 mm × 50 mm × 0.1 mm TNAs electrode and the other was 20 mm × 20 mm × 1 mm in net dimension with a Pt electrode (see Fig. 2a). Such a thin-layer reactor made it possible to keep the photoanode irradiated from both sides. The aqueous layer thickness at every sides of TNAs electrode in the reactor was about 0.2 mm and the distance between the working electrode and the center of UV light source (GE, 4 W, 254 nm) was 3 cm (see Fig. 2b). The organic solution (in total volume of 50 mL) was kept in a glass container connecting to the reactor. A peristaltic pump was applied to circulate the solution between the quartz cells and the solution container by a slender hose. The optimal flow velocity was controlled at 10 mL min^{-1} since relative stable degradation efficiency can be obtained as the flow velocity above 4 mL min^{-1} (Supporting Information Figure S3).

For the control experiment, a conventional reactor was set up and its parameters were summarized as follows: the effective volume of the reactor was 40 mm × 50 mm × 25 mm (cell thickness ~25 mm) in net dimension with a TNAs electrode of 40 mm × 50 mm × 0.1 mm. The 50 mL of 20–120 mg L^{-1} model tetracycline wastewater was kept in the reactor with vigorous agitation during the operation. The distance between the working electrode and the center of UV light source was 3 cm, and the aqueous layer thickness for illumination was 5 mm (see Fig. 2c). The radiation power from single-side illumination was controlled at 5 mW cm^{-2}.

In the further studies, an additional UV lamp was fixed in the symmetrical position at the other side of the thin-layer reactor (see Fig. 2b). The radiation power was controlled at 5 or 10 mW cm^{-2} as required and the dimension of reactor was chose at 40 mm × 50 mm × 0.5 mm or 80 mm × 50 mm × 0.5 mm with the corresponding TNAs electrode. 50 mL of 100–400 mg L^{-1} model tetracycline wastewater was kept in the thin-layer reactor with flow velocity of 10 mL min^{-1}.

Fig. 1. UV–visible spectra of tetracycline: (a) UV–visible spectrum and molecular structure of tetracycline, (b) calibration curve of tetracycline and (c) UV–visible spectra of tetracycline at different time intervals during the PEC process.

Fig. 2. Schematic diagram of the TNAs based thin-layer PEC reactor (a, b) and the conventional PEC reactor (c). In the comparative experiment, the TNAs electrode in each reactor was used as the working electrode and placed 3 cm away from UV lamp for singe side illumination, whereas both-side illumination was applied for the extended studies in the thin-layer PEC reactor.

2.5. Photoelectrochemical experiment

The photoelectrochemical experiments were performed using a three-electrode system with a platinum foil counter electrode, a saturated Ag/AgCl reference electrode and a TNAs working electrode. The potential and current of the working electrode were controlled by an electrochemical workstation (CH Instruments Inc. USA, CHI 660C). The polarization dark current and photocurrent response were measured in 20 mg L^{-1} tetracycline solution (0.1 M Na$_2$SO$_4$ solution as support electrolyte) under UV lamp illumination of 5 mW cm^{-2}. The photoelectrochemical properties on each side of the TNAs electrode were tested, respectively.

2.6. Degradation experiments

The PEC experiments were performed in the proposal reactors (as shown in Fig. 2). The supplied voltage was controlled using a power supply; UV lamps (GE, 4 W, 254 nm) were chosen as UV light source. The PC experiment was performed by using the same system without applying an external potential. The EC experiment was performed without UV illumination and the photolysis process was done with UV light alone.

2.7. Chemical analysis

The concentration of tetracycline was measured using a UV spectrophotometer (2102-PC, Shanghai Unico Co., China) at the wavelength of 355 nm [44]. The calibration curve of tetracycline determined at 355 nm and its linear equation was shown in Fig. 1. The pH value was measured with a PHS-3C pH meter (Shanghai Leici Apparatus Manufactory, Shanghai, China). The COD determination of the reaction solutions were carried out according to Refs. [24,25].
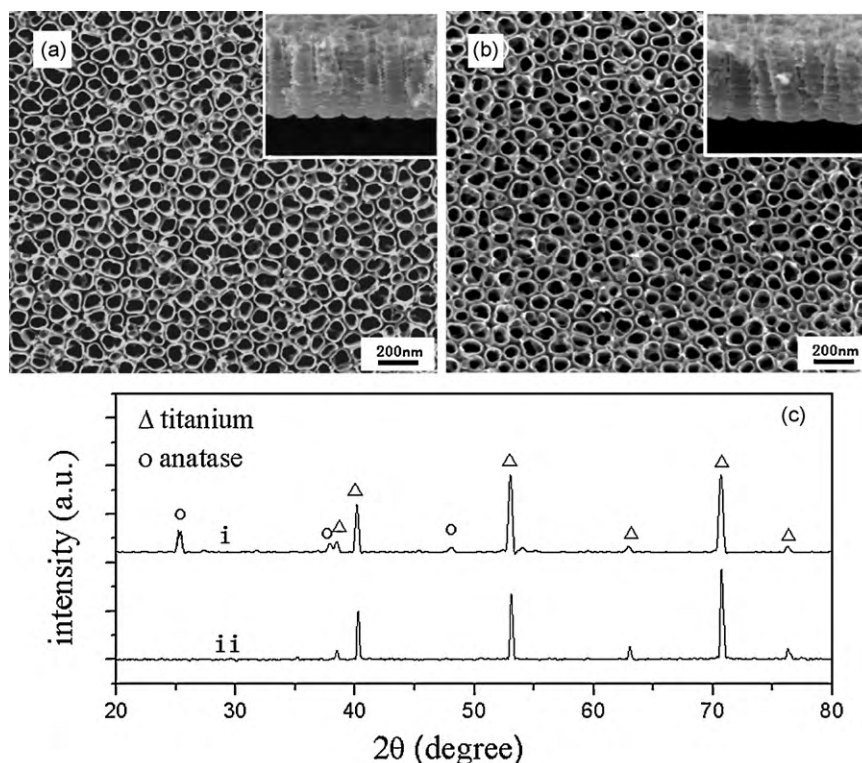
3. Results and discussion

The FE-SEM images of the front and back sides of the resulting TiO$_2$ nanotube arrays electrode are shown in Fig. 3. It can be observed from Fig. 3a and b that the nanotubes are highly ordered and well aligned, with the diameter of ∼100 nm and wall thickness of ∼10 nm [23]. Observing from the cross-section, the nanotubes are ∼420 nm in length and closely combined to the barrier layer. The surface scanning shows that the titania nanotubes were covered uniformly on both sides of the titanium foil. The short TNAs appears to be more robust and ordered compared with the long TNAs, thus, they can offer higher activity and stability in the long term usage for the degradation of organic compound.

The X-ray diffraction (XRD) patterns of the as-annealed TNAs electrode are shown in Fig. 3c. The nanotube without calcinations maintained an amorphous structure in Fig. 3c (ii), while the amorphous regions were gradually crystallized to form anatase phases via the calcinations at 500 °C in Fig. 3c (i). It can be seen from pattern a that the sample possesses characteristic peaks at 25.35° (1 0 1), 38.1° (0 0 4), and 48.2° (2 0 0) for the anatase phase. The titanium peaks can also be found owing to the Bragg reflection of Ti substrate.

To study the photoelectrochemical response of TNAs on each side of electrode, cyclic sweep photovoltammetry was applied in 0.1 M Na$_2$SO$_4$ supporting electrolyte under UV irradiation. The test was carried out in a three-electrode configuration and the results are shown in Fig. 4. It can be seen that the photocurrent increases with potential until reaching the saturated current; when the potential is above the oxygen releasing potential, the current increases in proportion with potential, showing the characteristic of conductive materials.

Comparing with the photocurrent obtained from the front side (Fig. 4a), the back side illumination (Fig. 4b) demonstrated similar photoelectrochemical response, implying that the entire surface of the electrode is covered with the homogeneous nanotubes. In other
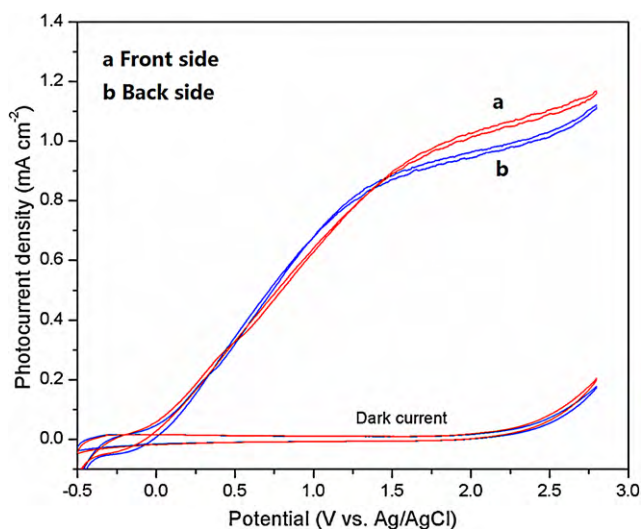
Fig. 3. FE-SEM top-view and corss-section (inset) of titania nanotube arrays on front of electrode (a) and back of electrode (b), XRD patterns of the titania nanotube arrays (c).
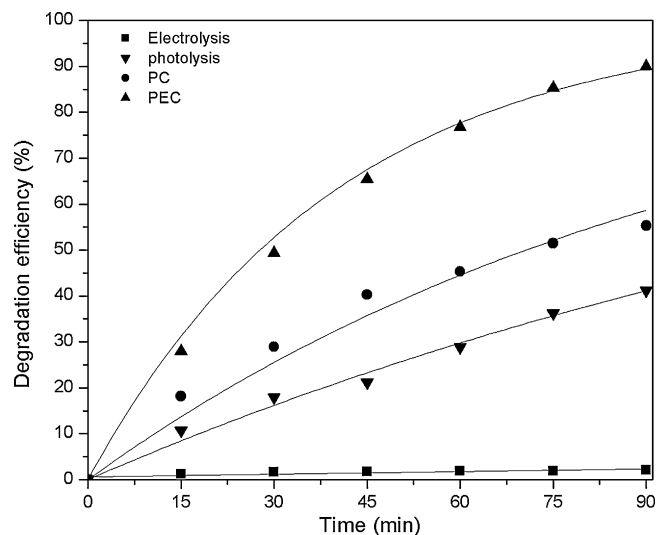
words, illuminated by both sides, the photogenerated current of TNAs electrode could double in PEC process; hence higher photo-catalytic reactivity can be obtained using this kind of electrode. The value of dark current was so small that it can be neglected.

Tetracycline was degraded under various processes such as photodegradation, photocatalysis (PC), electrolysis (EC), and photo-electrocatalysis (PEC) and the experimental results are summarized in Fig. 5. It can be seen that almost no tetracycline can be directly degraded by only applying the electrolysis under +1.0 V bias; and UV photolytic reaction only resulted in a removal ratio of 28.8% within 1 h. Compared to direct UV irradiation, the TNAs electrode
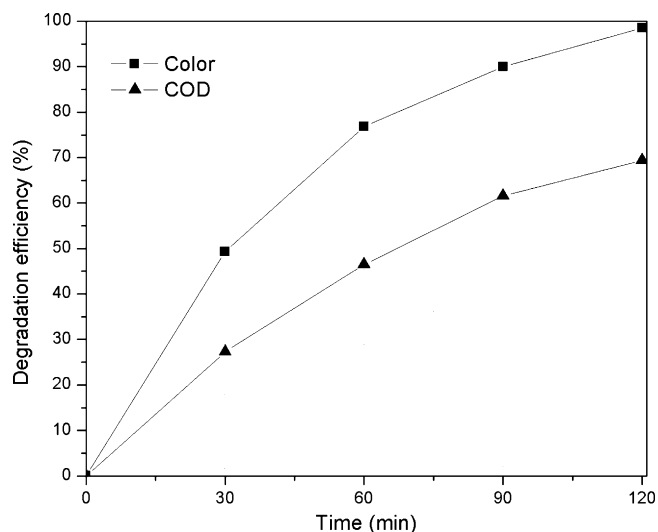
(without bias supply) degraded 45.3% of the tetracycline in the same time. However, it is easily observed from Fig. 5 that the PEC process obtained the removal rate of 76.8% under the same con-ditions. The TNAs electrode has been approved to be an excellent photoanode in the previous reports [20–22] since its advantage of fast electron transfer. When the given electric bias was supplied to the photocatalyst, it promoted the separation of photogener-ated holes and electron. This charge separation prevented the photoinduced electron and the hole from recombination and conse-quently leads to higher degradation efficiency. In short, electrolysis

Fig. 4. Photocurrent density versus applied potential (V vs. Ag/AgCl) of the TNAs on each side of electrode: (a) front side of the electrode, (b) back side of the electrode (experimental condition: 0.1 M Na_2SO_4 and light intensity 5 mW cm^{-2}).
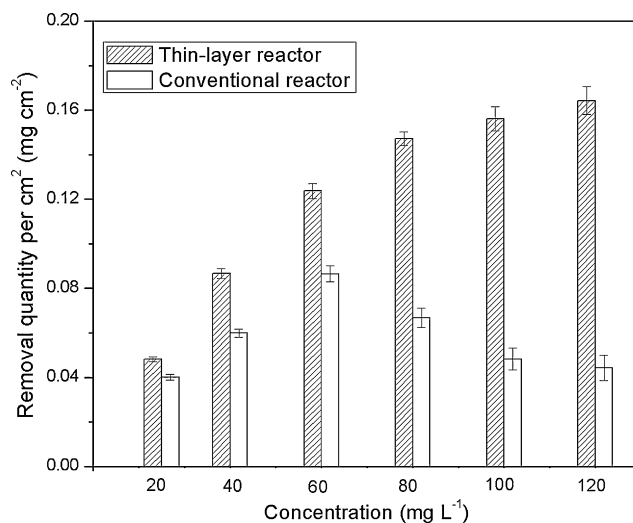

Fig. 5. Decolorization of tetracycline using different process in thin-layer reactor (experimental condition: natural pH 4.2, total 50 mL of 20 mg L^{-1} initial concentra-tion of tetracycline, 0.1 M Na_2SO_4, +1.0 V bias potential, light intensity 5 mW cm^{-2} and irradiation time 90 min).

Fig. 6. Color and COD removal of 20 mg L^{-1} TC by thin-layer reactor (experimental condition: natural pH 4.2, total 50 mL of 20 mg L^{-1} initial concentration of tetracycline, 0.1 M Na$_2$SO$_4$, +1.0 V bias potential, light intensity 5 mW cm^{-2} and irradiation time 120 min).

Fig. 7. Absolute quantity of tetracycline removed by each cm^2 electrode surface area using thin-layer PEC and conventional PEC procedure to treat tetracycline solutions at different concentration levels (experimental condition: bias potential +2.0 V, pH 8.0, single-side illumination, total 50 mL tetracycline solution, 0.1 M Na$_2$SO$_4$, light intensity 5 mW cm^{-2} and irradiation time 1 h).

or photolysis only plays a very insignificant role for tetracycline degradation in the PEC process. Fig. 6 shows that the color of tetracycline was almost totally removed in 120 min, whereas ~31.6% of COD was still present in the solution. Observing from Fig. 1c, the absorption peaks of tetracycline in the ultraviolet band were gradually decreasing. After 120 min degradation, the absorption peaks were almost disappeared. Since no new absorption peaks were formed during the degradation process, it can be deduced that the tetracycline molecules might be mineralized into CO$_2$ and H$_2$O and some small organic molecules during the PEC process. The effect of pH and bias potential on the PEC degradation of tetracycline was also investigated. The optimum bias potential and value of pH was chose at 2.0 V and 8.0, respectively. Accordingly, the PEC removal rate of tetracycline reached 96.4% within 1 h treatment (Supporting Information Figures S1 and S2).

Individual model tetracycline wastewater, with the concentration ranging from 20 to 120 mg L^{-1}, was treated by thin-layer PEC and conventional PEC under single-side illumination. The results of the removal rate are listed in Table 1. The thin-layer PEC removed rate of tetracycline reached 96.4–54.8% within 1 h, while only 80.4–14.6% by conventional PEC under the same conditions. It also can be seen from Table 1 that the ratio of their removal rate between thin-layer reactor and conventional reactor apparently increased with the solution concentration, implying that the oxidation capability of the thin-layer PEC is more stable in the high concentrated solution. Fig. 7 shows the absolute quantity of tetracycline removed by each cm^2 electrode surface area when applying the two types of PEC method to treat tetracycline solution at different concentration within 1 h. With tetracycline concentration increasing from 20 to 120 mg L^{-1}, tetracycline removed by thin-layer reactor steadily

increased, whereas the maximum amount of tetracycline removed by the conventional reactor was 60 mg L^{-1}. Beyond that concentration, tetracycline removal decreased. The main reason for the undesirable performance of the conventional reactor when treating the high-concentration solution is that the UV radiation had been mostly absorbed by the sample solution; without light transmission almost, and then the conventional PEC process actually became a weak electrolysis procedure. The effect was also demonstrated by the measurement of the apparent quantum efficiency of the two PEC processes (the calculation procedure was shown in supporting materials). As given in Table 2, it is evident that the apparent quantum efficiency of the PEC process almost kept constant regardless of the different concentration levels of the tetracycline in the thin-layer reactor. In contrast, it decreased sharply in the conventional reactor as the concentration of organic compounds increased. These results approved that the thin layer structure actually reduced the absorption of light by the solution. As well known, higher irradiation intensity provides higher photocurrent in the electrode in leading to more photogenerated holes in the reaction. Therefore, excellent photocatalytic activity is benefited from effectively utilization of photons in thin-layer reactor. In contrast, conventional reactor cannot avoid great loss of light intensity, especially in treatment of high concentration solution. This means that the thin-layer PEC reactor can be readily applied to the treatment of the high concentration organics without influencing its apparent quantum efficiency.

Apart from the property of reactor, the irradiation area of electrode, irradiation power and solution concentration, the three factors, also can greatly influence the treatment capacity. Different from the conventional reactor, the thin-layer PEC reactor has

Table 1
The degradation of tetracycline in thin-layer reactor and conventional reactor within 1 h treatment under single-side illumination (light intensity 5 mW cm^{-2}).

C_0 (mg L^{-1})	(I) Thin-layer PEC (% removal)	(II) Conventional PEC (% removal)	Ratio (I/II)
20	96.4 ± 1.7	80.4 ± 1.5	1.20
40	86.6 ± 2.0	59.9 ± 1.8	1.45
60	82.5 ± 2.4	50.7 ± 2.1	1.63
80	73.6 ± 1.5	33.4 ± 2.3	2.21
100	62.5 ± 2.3	19.3 ± 2.1	3.23
120	54.8 ± 2.1	14.6 ± 1.9	3.71

Table 2
The quantum efficiency of degradation in the different model tetracycline wastewater using conventional reactor or thin-layer reactor (light intensity 5 mW cm^{-2}).
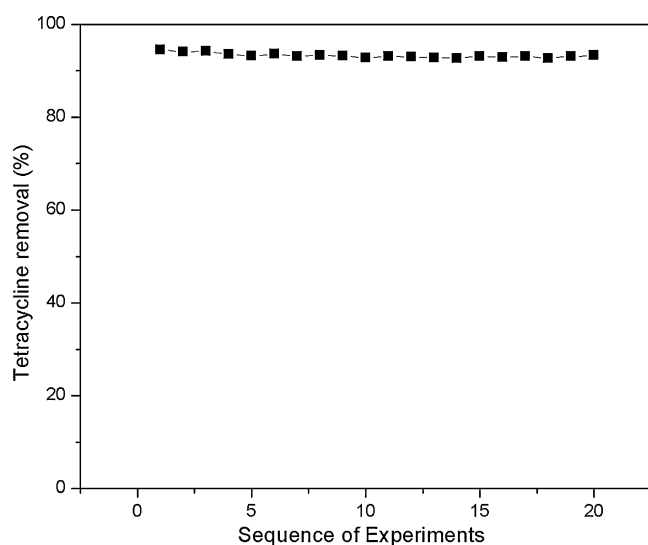
Concentration (mg L^{-1})	Quantum efficiency of degradation (%)	
	Conventional reactor	Thin-layer reactor
20	20	21.8
40	12.6	21
80	5.93	20.3
120	1.5	19.6

Table 3
The degradation of tetracycline by thin-layer PEC under single or double side illumination (dimension of electrode used in the experiment is 40 mm × 50 mm × 0.1 mm for run 1–2 and 80 mm × 50 mm × 0.1 mm for run 3–7, respectively).

Run	C_0 (mg L^{-1})	Illumination	Light intensity (mW cm^{-2})	Time needed after 90% degradation (min)
1	100	Single-side	5	100
2	100	Double-side	5	47
3	100	Singe-side	5	47
4	100	Double-side	5	22
5	100	Double-side	10	16
6	200	Double-side	10	36
7	400	Double-side	10	52

the advantage in effective utilization of double-faced TNAs electrode without being worried about the absorption of irradiation intensity. Moreover, the reactor can avoid volume restrictions of the solution container so that larger TNAs electrode can be utilized. In this experiment, 50 mL of 100–400 mg L^{-1} model tetracycline wastewater was treated using different experimental parameters. For the initial concentration of 100 mg L^{-1} tetracycline solution, it can be seen from Table 3 that it took almost 100 min to achieve 90% degradation under single-side illumination; whereas the time was shortened by approx. 50% under both-side irradiations, and further by approx. 75% when doubling the area of the TNAs electrode. It also can be seen from Table 3 (run 4–5) that the increase of light intensity from 5 to 10 mW cm^{-2} could further shorten the time needed from 22 to 16 min when other parameters were kept the same. This result shows that the thin-layer reactor can make full use of high irradiation power to treat organic solution in very short time. In order to estimate degradation efficiency for high concentration tetracycline solution, the thin-layer reactor was used to treat 200 and 400 mg L^{-1} tetracycline solution, respectively. Observing from Table 3 (run 6 and 7), it took only 36 or 52 min to degrade 90% of tetracycline under the light intensity of 10 mW cm^{-2} by double-side illumination, respectively. This shows that the designed thin layer structure can provide a large catalyst surface area per unit reactor volume; meanwhile, double-side illuminations further enlarged the catalyst surface area on a single electrode, resulting in much higher degradation efficiency in treatment of organics.

Fig. 8. Durability of TNAs electrode for treatment of high concentration of tetracycline solution in thin-layer reactor (experimental condition: bias potential +2.0 V, pH 8.0, double-side illumination, total 50 mL of 400 mg L^{-1} initial concentration of tetracycline solution, 0.1 M Na$_2$SO$_4$, light intensity 10 mW cm^{-2} and irradiation time 1 h).

Fig. 8 shows the durability of TNAs electrode for treatment of high concentration of tetracycline solution during a series of 20 identical tests in thin-layer reactor. The experiment was carried out under the condition: 50 mL of 400 mg L^{-1} tetracycline, 0.1 M Na$_2$SO$_4$ as electrolyte, irradiation time of 1 h, light intensity of 10 mW cm^{-2} and both-side illumination.

As can be seen from Fig. 8, the PEC results of the 20 repeated experiments for degradation of tetracycline in 1 h shows that the degradation efficiencies were rather stable with an average degradation efficiency of 93.1 ± 1.3%. This indicates that TNAs electrode processes excellent stability and reliability in the thin-layer reactor for the treatment of high concentration solutions.

4. Conclusion

A novel thin-layer photoelectrocatalytic (PEC) reactor with double-faced titania nanotube arrays (TNAs) electrode was designed and then applied to degrade tetracycline solution. The configuration of thin layer of reactor offers pretty thin aqueous layer in a cycled system during the PEC process, thus, can obtain much higher degradation efficiency in comparison to the traditional bulk reactor. Results also show that thin-layer PEC reactor can efficiently treat high concentration organic solution and possess excellent stability and reliability during the serial experiments.

Benefited from convenient fabrication process of double-side TNAs electrode, the new reactor can use much larger TNAs electrode to increase its treatment capacity; similarly, multi-reactor can be connected in series or parallel for the same purpose. By continuous improving the configuration and photoanode of the reactor, this new reactor can be developed into a kind of convenient device with superior performance to treat various biorefractory environmental organic pollutants.

Appendix A. Supplementary data

Supplementary data associated with this article can be found, in the online version, at doi:10.1016/j.apcatb.2010.05.024.

References

[1] A. Fujishima, K. Honda, Nature 238 (1972) 37–38.
[2] R.A. Damodar, K. Jagannathan, T. Swaminathan, Solar Energy 81 (2007) 1–7.
[3] A. Rachel, M. Subrahmanyam, P. Boule, Appl. Catal. B: Environ. 37 (2002) 301–308.
[4] Z. Miao, D. Xu, J. Ouyang, G. Guo, X. Zhao, Y. Tang, Nano Lett. 2 (2002) 717–720.
[5] B. Ma, J.K.L. Goh, T.J. White, J. Electrochem. Soc. 154 (2007) D557–D561.
[6] A. Yuwono, B. Liu, J. Xue, J. Wang, H.I. Elim, W. Ji, Y. Li, T.J. White, J. Mater. Chem. 14 (2004) 2978–2987.
[7] S.U.M. Khan, M. Al-Shahry, W.B. Ingler, Science 297 (2002) 2243–2245.
[8] R. Asahi, T. Morikawa, T. Ohwaki, K. Aoki, Y. Taga, Science 293 (2001) 269–271.
[9] M. Wang, D.J. Guo, H.L. Li, J. Solid State Chem. 178 (2006) 1996–2000.
[10] D. Gong, C.A. Grimes, O.K. Varghese, W. Hu, R.S. Singh, Z. Chen, E.C. Dickey, J. Mater. Res. 16 (2001) 3331–3334.
[11] J.M. Macak, H. Tsuchiya, A. Ghicov, K. Yasuda, Curr. Opin. Solid State Mater. 11 (2007) 3–18.
[12] A. Ghicov, P. Schmuki, Chem. Commun. (2009) 2791–2808.
[13] G.K. Mor, K. Shankar, M. Paulose, O.K. Varghese, C.A. Grimes, Nano Lett. 6 (2006) 215–218.
[14] O.K. Varghese, M. Paulose, K. Shankar, G.K. Mor, C.A. Grimes, J. Nanosci. Nanotechnol. 5 (2005) 1158–1165.
[15] J.M. Macak, H. Tsuchiya, A. Ghicov, P. Schmuki, Electrochem. Commun. 7 (2005) 1133–1137.
[16] S. Funk, B. Hokkanen, U. Burghaus, Nano Lett. 7 (2007) 1091–1094.

[17] I. Paramasivam, J.M. Macak, P. Schmuki, Electrochem. Commun. 10 (2008) 71–75.
[18] J.M. Macak, M. Zlamal, J. Krysa, P. Schmuki, Small 3 (2007) 300–304.
[19] M. Zlamal, J.M. Macak, P. Schmuki, J. Krýsa, Electrochem. Commun. 9 (2007) 2822–2826.
[20] X. Quan, S.G. Yang, X.L. Ruan, H.M. Zhao, Environ. Sci. Technol. 39 (2005) 3770–3775.
[21] Z.H. Zhang, Y. Yuan, G.Y. Shi, Y.J. Fang, L.H. Liang, H.C. Ding, L.T. Jin, Environ. Sci. Technol. 41 (2007) 6259–6263.
[22] H.F. Zhuang, C.J. Lin, Y.K. Lai, L. Sun, J. Li, Environ. Sci. Technol. 41 (2007) 4735–4740.
[23] J. Bai, B.X. Zhou, L.H. Li, Q. Zheng, Y.B. Liu, J.H. Shao, X.Y. Zhu, W.M. Cai, J. Mater. Sci. 43 (2008) 1880–1884.
[24] Q. Zheng, B.X. Zhou, J. Bai, L.H. Li, Z.J. Jin, J.L. Zhang, J.H. Li, Y.B. Liu, W.M. Cai, X.Y. Zhu, Adv. Mater. 20 (2008) 1044–1049.
[25] J.L. Zhang, B.X. Zhou, Q. Zheng, J.H. Li, J. Bai, Y.B. Liu, W.M. Cai, Water Res. 43 (2009) 1986–1992.
[26] Y.B. Liu, J.H. Li, B.X. Zhou, J. Bai, Q. Zheng, J.L. Zhang, W.M. Cai, Environ. Chem. Lett. 7 (2009) 363–368.
[27] Y.B. Liu, B.X. Zhou, J. Bai, J.H. Li, J.L. Zhang, Q. Zheng, X.Y. Zhu, W.M. Cai, Appl. Catal. B-Environ. 89 (2009) 142–148.
[28] J. Bai, J.H. Li, Y.B. Liu, B.X. Zhou, W.M. Cai, Appl. Catal. B-Environ., doi:10.1016/j.apcatb.2010.01.020.
[29] Y.B. Liu, B.X. Zhou, J.H. Li, X.J. Gan, J. Bai, W.M. Cai, Appl. Catal. B-Environ. 92 (2009) 326–332.
[30] Y.B. Liu, X.J. Gan, B.X. Zhou, B.T. Xiong, J.H. Li, C. Dong, J. Bai, W.M. Cai, J. Hazard. Mater. 171 (2009) 678–683.
[31] T. An, Y. Xiong, G. Li, C. Zha, X. Zhu, J. Photochem. Photobiol. A 152 (2002) 155–165.
[32] S. Horikoshi, Y. Satou, H. Hidaka, N. Serpone, J. Photochem. Photobiol. A 146 (2001) 109–119.
[33] T. An, Y. Xiong, G. Li, X. Zhu, G. Sheng, J. Fu, J. Photochem. Photobiol. A 181 (2006) 158–165.
[34] M. Noorjahan, M.P. Reddy, V.D. Kumari, B. Laveĭdrine, P. Boule, M. Subrahmanyam, J. Photochem. Photobiol. A: Chem. 156 (2003) 179–187.
[35] J. Alex, N.C. Holm, S.G. Rönner-Holm, Water Res. 37 (2003) 1125–1135.
[36] M.V. Shankar, S. Anandan, N. Venkatachalam, B. Arabindoo, V. Murugesan, J. Chem. Technol. Biotechnol. 79 (2004) 1279–1285.
[37] J. Kulas, I. Rousar, J. Krýsa, J. Jirkovský, J. Appl. Electrochem. 28 (1998) 843–853.
[38] Y.L. Xu, Y. He, X.D. Cao, D.J. Zhong, J.P. Jia, Environ. Sci. Technol. 42 (2008) 2612–2617.
[39] Y.L. Xu, Y. He, J.P. Jia, D.J. Zhong, Y. Wang, Environ. Sci. Technol. 43 (2009) 6289–6294.
[40] H.J. Zhao, D. Jiang, S. Zhang, W. Wen, J. Catal. 250 (2007) 102–109.
[41] H.J. Zhao, D. Jiang, S. Zhang, K. Catterall, R. John, Anal. Chem. 76 (2004) 155–160.
[42] O.K. Dalrymple, D.H. Yeh, M.A. Trotz, J. Chem. Technol. Biotechnol. 82 (2007) 121–134.
[43] N. Bolong, A.F. Ismail, M.R. Salim, T.A. Matsuura, Desalination 239 (2009) 229–246.
[44] C. Reyes, J. Fernandez, J. Freer, M.A. Mondaca, C. Zaror, S. Malato, H.D. Mansilla, J. Photochem. Photobiol. A: Chem. 184 (2006) 141–146.